Numerical Simulation and Parametric Study of Penetration Effect for an Ogive-Nose-Shaped Projectiles Against Concrete Target

Patel Yash Bipinbhai, P. C. Tewari, Mukesh Kumar, and Pravendra Kumar

1 Introduction

Kinetic energy projectile is a weapon mostly used in defence and military applications which contains an explosive charge. It works on a principle to attain a high velocity, generally up to hypervelocity and strike the target material, converting kinetic energy into shock waves and heat. Hence, they are designed in such a way to defeat military bunkers, high aircraft shelters, deep buried targets, etc. Penetration of projectile into a concrete target is an interesting topic for many scholars. Many researchers were investigating various parameters of penetration by calculating projectile depth of penetration, the effect of concrete target diameter on the depth of penetration, etc. Forrestal [1] derived an empirical formula to examine the depth of penetration into the concrete target. From the last three decades, three major techniques were castoff to envisage the interaction of projectile with concrete material. Concrete is remembered because of its low cost and wide availability. It was well defined by its unconfined compressive strength and its ubiquity, but has certain demerits like brittleness, weak in tension, inelastic deformation before failure, etc. Due to the formation of cracks, spalling and scabbing on the target arise erratically. A continuous analysis on the physical and mechanical behaviour of concrete and its composition at the macroscopic level is obedient as concrete is a complex material widely used in structural applications such as bunkers, buildings, dams. The reinforced concrete, i.e. a mixture of steel and concrete, is used to enhance the bending stress of concrete and improve its tensile strength.

P. Y. Bipinbhai (✉) · P. C. Tewari
Department of Mechanical Engineering, National Institute of Technology, Kurukshetra, Haryana 136119, India
e-mail: yashbpatel1005@gmail.com

M. Kumar · P. Kumar
Terminal Ballistics Research Laboratory, Defence Research and Development Organisation, Chandigarh, India

P. K. Rakesh et al. (eds.), *Advances in Engineering Design*, Lecture Notes in Mechanical Engineering, https://doi.org/10.1007/978-981-33-4018-3_33

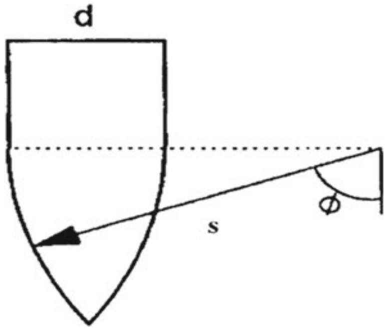

Fig. 1 Design of ogive-nose [10]

Rajput et al. [5] studied the effect of plain and reinforced concrete by impacting hard ogive nose steel projectile at a tremendous velocity. Here, crater diameter was estimated and residual versus impact velocity was observed and related amongst these two targets. Wu et al. [6] prophesied the velocities which are remained as a residue of a projectile afterwards normally perforating the thin UHP-SFRC barriers. Wu et al. [7] analysed high-velocity penetration of the concrete target material with different shapes of a projectile using two constituents. Over here, penetration depth and trajectory stability of these projectiles were analysed. Outcomes disclosed that double-nose projectile had specific drag reduction, high penetration ability. In the interim, projectile with groove-tapered owned good trajectory stability as its curved part had tapering shank which helped in restoring moment for stabilization. Feng et al. [8] replicated sets of experiments to study the effect of thick PCT to high-velocity penetration of an alloy steel projectiles by varying its striking velocities. The crater diameter increased linearly with the striking velocity. Oucif and Mauludin [9] evaluated the geometric modelling of high-speed impact of ogive nose-shaped projectile against reinforced concrete panel using Johnson–Holmquist damage model.

In the facts mentioned above, the present work is conducted by impacting conventional ogive-nose-shaped projectiles, as shown in Fig. 1 with two shapes of the projectile of different CRH and penetrating into the concrete target. Moreover, the penetration depth and the crater damage on the impact face of the targets are analysed.

2 Numerical Simulation Tool

ANSYS AUTODYN user interface is an analytical tool required to model nonlinear dynamics of solids, fluids, gas, and its interaction. It is easy to use, fully integrated, and enable us to set up, run, and post-process given problems. AUTODYN has been functionalized in a vast range such as enhancing and designing of anti-armor systems, building protection in contradiction of blast marvels, risk identification in contrast to aircraft impact, material characterization lay open to impact and dynamic loading, drop test, etc.

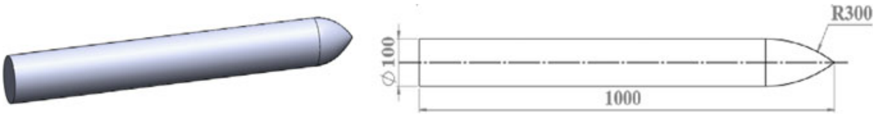

Fig. 2 Ogive-nose shape with 1.5 CRH

Table 1 Mixture ratio of M35 grade of concrete

Unconfined compressive strength (MPa)	Cement	Sand	Coarse aggregates
35	1	1.6	2.907

3 Design

3.1 Projectile

A 100-mm-diameter, 1-m-long ogive-nosed projectiles are designed for impacting the concrete target. They are machined from steel 4340 rods. Here, two projectiles of 1.5 and 3.0 CRH are tested against the concrete target. Ogive-nose CRH outlines the ratio of ogive radius to the projectile or shank diameter. Figure 2 simply shows the difference projectile nose shape. It is accelerated at an impact velocity of 350 m/s towards the target. Here, it is assumed that the projectile is kept rigid, i.e. deformation or damage free. Therefore, no failure criteria were applied to this material.

3.2 Concrete Target

In this study, plain concrete target (PCT) and reinforced concrete target (RCT) have taken as target materials. The material applied for the target is M35 grade of concrete, namely CONC-35 MPa; see Table 1.

Concrete is good in compression rather than tension. The reinforcement is suitable to provide strength against tension. Figures 3 and 4 display the front and isometric view of the reinforced concrete target. The thick PCT size of 500 × 500 × 1500 mm is modelled in ANSYS AUTODYN, and reinforcement is filled in case of RCT. The reinforcement material is preferred as cast iron.

3.3 FEM for Meshing

In the analysis, meshing is necessary to achieve accurate results. A fine mesh is required to compute complex problems. The finite element method (FEM) is the best numerical technique which generates fairly accurate solutions by discretizing a

Fig. 3 Front view of RCT

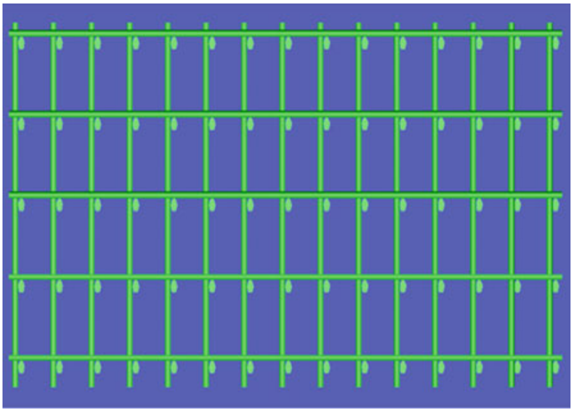

Fig. 4 Isometric view of RCT

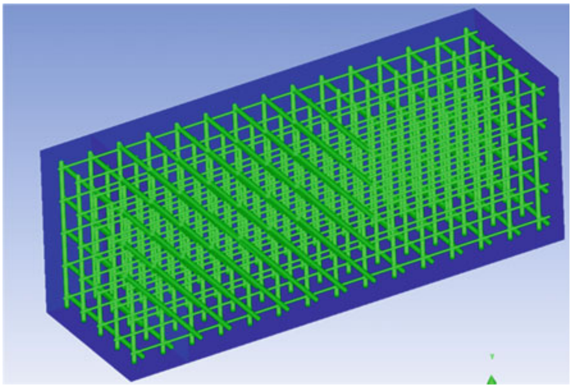

complicated problem into a small number of elements. The point connecting between them is defined by nodes and the complex system of these points, which produce a grid named as mesh. The element size for projectile mesh is 7 mm, as shown in Fig. 5 while that of the concrete target is 25 × 25 × 25 mm.

Fig. 5 Four-node tetrahedron projectile meshing

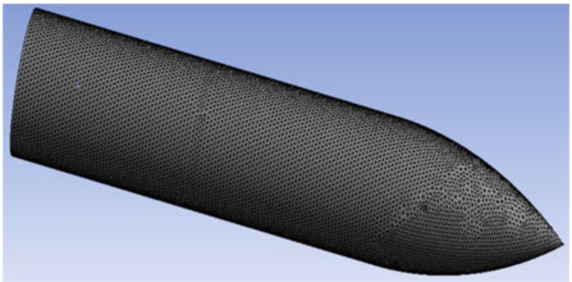

3.4 Material Model

Material model is distributed based on three major criteria:

(a) Equation of state
(b) Material strength model
(c) Material failure model

(a) **Equation of State (EOS)**
For projectile and reinforcement material, linear EOS criteria are used which express $P = f(\rho, e)$. Here, ρ = density and e = internal energy.
For concrete target, porous-alpha polynomial EOS is designed in AUTODYN due to its compaction and compressibility.

(b) **Material Strength Model**
Initially, all solid materials react elastically in nature, but over an extreme dynamic loading condition, they can extend to stress where it exceeds yield stress and then deforms plastically.
Johnson–Cook equation

$$\sigma = [\sigma_0 + B\epsilon^n] \times [1 + c(\epsilon/\epsilon_0)] \times [1 - \{(T - T_\mathrm{r}) / (T_\mathrm{m} - T_\mathrm{r})\}^m] \quad (1)$$

where σ = yield stress, σ_0 = static yield stress, B = hardening constant, n = hardening exponent, c = stress-rate constant, ϵ_0 = reference strain rate, T_m = melting point, T_r = reference temperature, m = thermal softening constant.

(c) **Material Failure Model**
Material may fail under high hydrodynamic loading conditions, resulting in the occurrence of crack. Considering in mind that concrete fails under tensile load rather than in compressive load, the failure model of the M35 grade of concrete is simulated under the hydrodynamic tensile failure criteria. The material model for projectile penetration into concrete target material is presented in Table 2.

4 Empirical Formulae

Numerical simulation results are compared with the empirical equation. Forrestal et al. formulated an equation to determine the DOP equation for an ogive-nose-shaped projectile penetrating M35 grade of the concrete target. The below-mentioned

Table 2 Material model

Material composition	EOS	Strength criteria	Failure criteria
SS 4340	Linear	Johnson–Cook	–
M35 grade of concrete	Porous-alpha	RHT concrete	RHT concrete
IRON–C.E	Linear	Johnson–Cook	–

Table 3 Calculated depth of penetration (DOP) for both nose shapes of projectiles

CRH	Mass (kg)	*N* value	DOP (mm)
1.5	58.336	0.2037	1135
3.0	56.72	0.1065	1152

penetration equation is obtained from post-test scrutiny of soil and concrete target material [1]. The penetration in concrete is subdivided into two definite processes, viz. formation of crater and tunnelling phenomena. By using this penetration equation, depth of penetration comes out and is revealed in Table 3.

$$P = \frac{m}{2\pi a^2 \rho N} \ln\left(1+\frac{N\rho V^2}{R}\right) + 4a \tag{2}$$

$$V^2 = \frac{mV_s^2 - 4\pi a^3 R}{m + 4\pi a^3 N\rho} \tag{3}$$

$$N = \frac{8\psi - 1}{24\psi 2} \tag{4}$$

$$\psi = \frac{r}{2a} \tag{5}$$

Here, P = depth of penetration, m = mass of projectile, ρ = target density, a = projectile radius, V_s = striking velocity, Ψ = calibre-radius-head (CRH), r = calibre-radius, R = empirical constant (410 MPa), N = nose shape factor.

5 Results and Discussions

The main objective of this study was to observe the behaviour between plain concrete and reinforced concrete and its effect on penetration depth and crater formation on the front as well as rear faces. Numerical simulation is conducting using below mentioned four cases of projectile, viz. shown in Table 4. Lagrange interaction is applied between projectile and concrete target. Figure 6 expresses the preliminary setup of complex problem interaction in AUTODYN-3D.

Table 4 Various cases of ogive-nose-shaped projectile

Case	Target	CRH value
I	PCT	1.5
II	RCT	1.5
III	PCT	3.0
IV	RCT	3.0

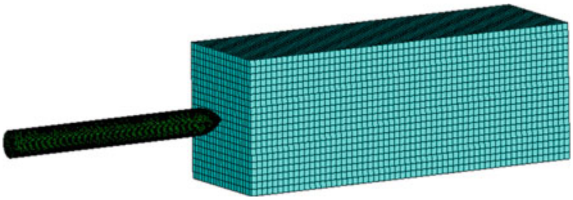

Fig. 6 Interaction using 1.5 CRH projectile

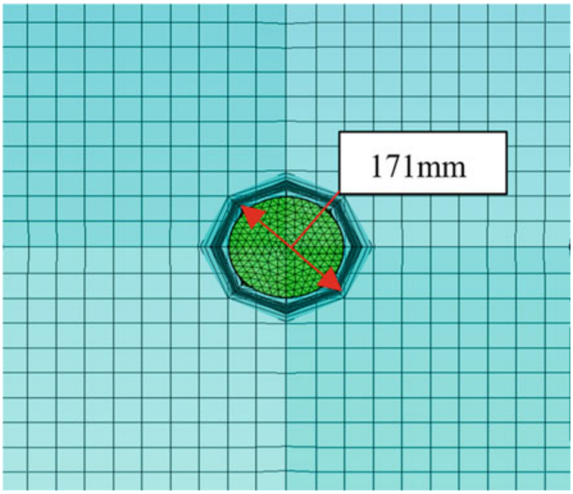

Fig. 7 Crater diameter at $t = 9.785$ ms (case-I)

Here, it is obtained results of crater diameter and penetration depth through numerical simulations along with their results is compared with empirical results.

5.1 Crater Diameter

Crater diameter is generated due to high-velocity impact of the projectile against the target material. Figures 7 and 8 describe these much value of crater diameter caused during penetration in target for all the cases. The figure illustrates the damage produced at the front face of plain as well as the reinforced concrete target.

5.2 Depth of Penetration (DOP)

The penetration depth or depth of penetration (DOP) for all these cases obtained from the AUTODYN is given in Figs. 9 and 10. The results are compared with the

Fig. 8 Crater diameter at $t = 8.002$ ms (case-II)

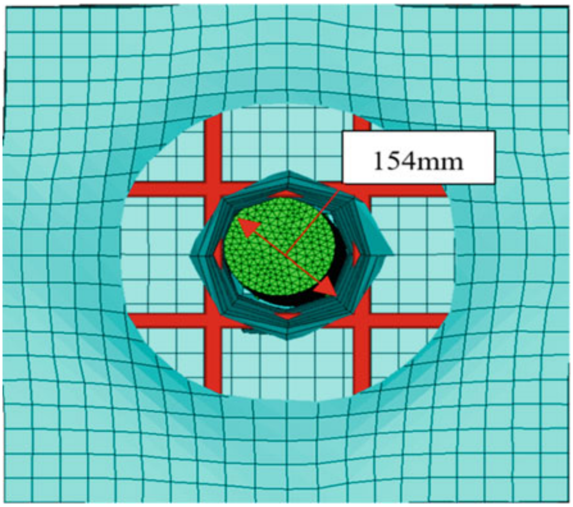

Fig. 9 Penetration depth at $t = 9.785$ ms (case-I)

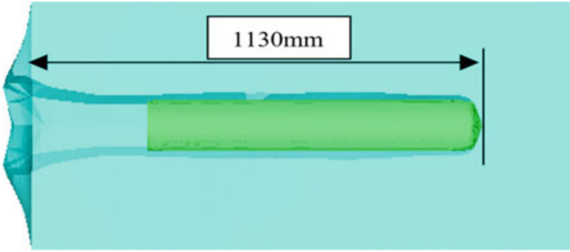

Fig. 10 Penetration depth at $t = 8.002$ ms (case-II)

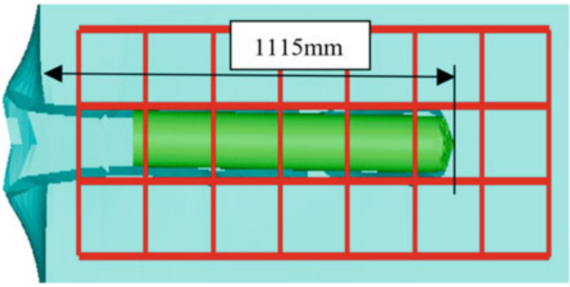

empirical approach, viz. known as Forrestal penetration equation. One observation was clarified that there is less variation in penetration depth in both RCT and PCT.

Finally, all these results are gathered and displayed as a bar chart shown in Fig. 11 which is appeared from the numerical simulation. Here, maximum and minimum DOP is achieved in PCT with 3.0 CRH projectile and RCT with 1.5 CRH projectile, respectively. PCT with 1.5 CRH projectile has maximum crater damage, while RCT

Fig. 11 Outcomes from numerical simulation

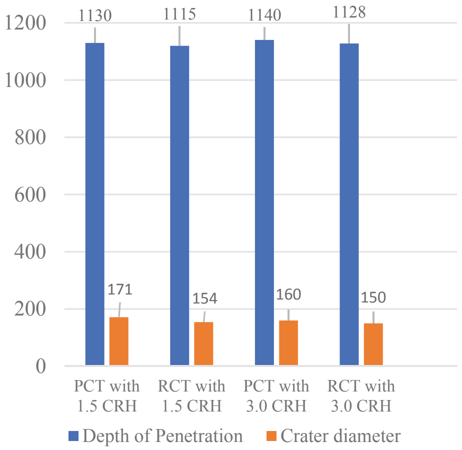

with 3.0 CRH projectile has least crater damage. Due to technical constraints, up to 7% of error is considerable in the value of the results of penetration when compared with empirical equations because of some limiting factors such as mesh size, meshing method, interactions, irrelevant selection of the material model.

6 Conclusion

From this paper, the multifaceted interaction of a projectile with target material is an interesting topic of research for ballisticians. From the simulation results, it may be concluded that by adding steel fibres in the concrete, there is an appreciable decrease in spalling and scabbing on the concrete target. Forrestal et al. [1] empirical formulae are used as a benchmark for comparing results with numerical simulation. The results obtained from the penetration equation are validated upright promise with the results of numerical simulation.

References

1. Forrestal MJ, Altman BS, Cargile JD, Hanchak SJ (1994) An empirical equation for penetration depth of ogive-nose projectiles into concrete targets. Int J Impact Eng 15(4):395–405
2. Frew DJ, Forrestal MJ, Cargile JD (2006) The effect of concrete diameter on projectile deceleration and penetration depth. Int J Impact Eng 32(10):1584–1594
3. Tham CY (2006) Numerical and empirical approach in predicting the penetration of a concrete target by an ogive-nosed projectile. Finite Elem Anal Des 42(14–15):1258–1268
4. Ulrika N, Kent G (2011) Comparative numerical studies of projectile impacts on plain and steel-fibre reinforced concrete. Int J Impact Eng 38(2–3):95–105
5. Rajput Abhishek R, Jakka BMP, Iqbal MA (2016) Experimental study of plain and reinforced concrete targets subjected to impact loading. Procedia Eng 144:124–131

6. Wu H, Peng Y, Fang Q, Gong ZM, Liu JZ (2016) Residual velocities of projectiles after normally perforating the thin Ultra-High-Performance steel fibre reinforced concrete slabs. Int J Impact Eng 97:1–9
7. Wu H, Zhang S, Zhang X, Liu J, Huang F (2017) High-velocity penetration of concrete targets with three types of projectiles: experiments and analysis. Lat Am J Solids Struct 14(9):1614–1628
8. Feng J, Li W, Li W, Song M, Sun W, Weng L (2018) Thick plain concrete targets subjected to high speed penetration of 30CrMnSiNi2A steel projectiles: tests and analyses. Int J Impact Eng 122:305–317
9. Oucif C, Mauludin LM (2019) Numerical modelling of high-velocity impact applied to reinforced concrete panel. Undergr Space 4(1):1–9
10. Chen XW, Li QM (2002) Deep penetration of a non-deformable projectile with different geometrical characteristics. Int J Impact Eng 27(6):619–637